Chemical Engineering Journal 162 (2010) 1057–1066

Contents lists available at ScienceDirect

Chemical Engineering Journal

journal homepage: www.elsevier.com/locate/cej

Energy and exergy analysis of an ethanol fueled solid oxide fuel cell power plant

Yannay Casas[a], Luis E. Arteaga[a,*], Mayra Morales[a], Elena Rosa[b], Luis M. Peralta[a], Jo Dewulf[c]

[a] Chemical Engineering Department, Central University of Las Villas, Road to Camajuaní Km 5.5., Santa Clara, c/p 54830 Villa Clara, Cuba
[b] Applied Chemistry Center, Central University of Las Villas, Road to Camajuaní Km 5.5., Santa Clara, c/p 54830 Villa Clara, Cuba
[c] Research Group ENVOC, Ghent University, Coupure Links 653, 9000 Ghent, Belgium

ARTICLE INFO

Article history:
Received 7 December 2009
Received in revised form 14 June 2010
Accepted 15 June 2010

Keywords:
Exergy
Efficiency
Fuel cell
Irreversibility
Steam reforming

ABSTRACT

A solid oxide fuel cell (SOFC) system integrated with an ethanol steam reforming unit is evaluated considering the first and second laws of thermodynamics. The ethanol reaction kinetic data and system architecture were developed in two previous communications. The irreversibility losses distribution and the plant energy and exergy efficiencies are studied at different reformer temperatures ($823 < T < 973$ K), water to ethanol molar ratios ($5 < R_{AE} < 6.5$) and fuel utilization factor ($0.7 < U_f < 0.9$). The post-combustion of the cell off gases for the heat recovery is also taken into account to maintain the system operation within the auto-sustainability boundaries. An increase of efficiency and irreversibility at the stack is reported when the reactants ratio is increased. The higher losses are placed at the steam reformer (280–350 kW) and the cell (400–590 kW) due to the combination of the chemical composition and stream conditions on chemical and physical components of the exergy.

1. Introduction

Fuel cells are considered the most efficient energetic system of the near future, since they can produce electricity without polluting the environment, and possess the necessary specific power, power density and durability to replace conventional internal combustion engines from their current applications [1]. In recent years, the solid oxide fuel cell (SOFC) running on pure hydrogen or crude gases has drawn great attention, due to its high efficiency and degree of integration even with turbine cycles [2–4]. SOFCs support internal conversion of light hydrocarbons, alcohols and carbon monoxide without using noble metals as electrodes [1,2,5].

A traditional method to study a power generation system is the energetic analysis applying the first law of thermodynamics; it has been widely used to asses the solid oxide fuel cells. However, it is clear that indeed, an exergetic analysis with exergy as the measure of the quality (useful part, transformable to work) of energy can be used to specify design conditions which are different from those resulting from the energy conservation law [6].

In a previous paper [7], the heat exchanger network synthesis of a SOFC fed directly with syngas produced in an ethanol external reformer, was reported. In that paper, the effect of the steam reforming kinetic pattern was taken into account and the pinch methodology was applied to minimize the use of utilities. Over the last few years, SOFC systems fed with ethanol, biomass, methane and hydrogen considering different forms of primary fuel conversion (reforming, partial oxidation, gasification) has been analyzed through exergy tools [8,9].

In this sense Douvartzides et al. [9] developed an energy–exergy analysis in order to optimize the operational conditions of a SOFC power plant, considering only the hydrogen oxidation within the fuel cell (Eq. (1)), and rejecting the effect of the cell losses, in situ methane reforming and carbon monoxide conversion. Moreover, Douvartzides et al. [8,9] did not take into account the effect of the kinetic pattern of the ethanol steam reforming (ESR) on syngas composition and instead they use the extent of the reaction (ε) as a measure of fuel conversion. The optimal condition was reached for a SOFC fuel utilization factor of 79.85%, an ethanol conversion of 100%, water to ethanol ratio 3:1 and no thermal integration was developed.

A more detailed model was reported by Hotz et al. [6], which performed the optimization of the exergy efficiency considering an analytical model of a microsolid fuel cell system fed with liquid butane (non-renewable fuel) previously reformed in a partial oxidation (POX) reactor. 1D and 2D extended polarization models were used to study the cell losses and also to determine the convective mass and heat transfer on cell channels and from the cell to the environment. The electrochemical oxidation of hydrogen was used as the only source of electrons in a not thermal integrated system:

$$\begin{array}{l} H_2 + O^{2-} \rightarrow H_2O + 2e^- \\ (1/2)O_2 + 2e^- \rightarrow O^{2-} \\ \hline H_2 + (1/2)O_2 \rightarrow H_2O \end{array} \quad \text{Electrochemical conversion of hydrogen} \quad (1)$$

* Corresponding author. Tel.: +53 422 81164; fax: +53 422 81608.
E-mail address: luiseap@gmail.com (L.E. Arteaga).

1385-8947/$ – see front matter © 2010 Elsevier B.V. All rights reserved.
doi:10.1016/j.cej.2010.06.021

Nomenclature

A_t	flow area of reformer (m^2)
Atc	heat transfer area (m^2)
CPR	compressor pressure ratio
e_i^{ch}	molar chemical exergy of species i (kJ $kmol^{-1}$)
e_i^{ph}	molar physical exergy of species i (kJ $kmol^{-1}$)
e_i^o	standard chemical exergy of species (kJ $kmol^{-1}$)
e_i	total exergy of each chemical species (kJ $kmol^{-1}$)
E_C	exergy destruction in the compressor (kW)
E_{ESR}	exergy destruction in the reformer (kW)
E_{HEX}	exergy destruction in the heat exchanges (kW)
E_{in}	activation energy (kJ $kmol^{-1}$)
E_{irrev}	exergy destruction (kW)
E_{PC}	exergy destruction in the post-combustion (kW)
E_{SOFC}	exergy destruction in the SOFC (kW)
f^{in}	inlet molar flow of component j (kmol s^{-1})
f^{out}	outlet molar flow of component j (kmol s^{-1})
F	Faraday constant (96,487 C mol^{-1})
F_{H_2}	hydrogen flow exiting the reactor (kmol s^{-1})
$F_{ethanol}^{in}$	ethanol flow feed to the reactor (kmol s^{-1})
H	molar absolute enthalpy (kJ mol^{-1})
H_o	molar enthalpy at reference state (kJ mol^{-1})
HHV	higher heating value (kJ $kmol^{-1}$)
I_{SOFC}	cell current (A)
J	current density (A m^{-2})
$J_{o,i}$	exchange current density (A m^{-2})
K_{in}	pre-exponential factor (8.542 kmol m^{-1} s^{-1} $(bar_{abs}^2)^{-1}$
LHV	lower heating value (kJ $kmol^{-1}$)
$p(H_2O)$ and $p(CH_4)$	partial pressure of water and methane (bar)
P_{SOFC}	cell power output (kW)
Q_j	heat duty of component j (kW)
R	universal gas constant (kJ K^{-1} $kmol^{-1}$)
R_{AE}	water/ethanol molar ratio
r_{zi}	reaction rate for component i at the reformer (kmol s^{-1} kg^{-1})
S	molar absolute entropy (kJ mol^{-1} K^{-1})
S_o	molar entropy at reference state (kJ mol^{-1} K^{-1})
S_{SOFC}	SOFC area (m^2)
T_g^{in}	inlet gases temperature of reformer (K)
T_g^{out}	outlet gases temperature of reformer (K)
T_j	temperature of component j (K)
U	heat transfer coefficient (kW m^2 K^{-1})
U_f	fuel utilization coefficient
V_{ideal}	Nernst potential (V)
V_{SOFC}	single cell voltage (V)
W	power (kW)
x	mole fraction of species
X	compound conversion
Y_{H_2}	hydrogen yield (kmol of produced H_2/kmol of ethanol fed to the reactor).
z	distance on the length reformer (m)

Greeks letters

η_{exergy}	exergy efficiency (%)
η_{energy}	energy efficiency (%)
η_{act}	activation overpotential (V)
η_{conc}	concentration overpotential (V)
η_{ohm}	ohmic overpotential (V)
ε	porosity
α_i	stoichiometric coefficient for component i
$\eta_{p,c}$	compressor polytropic efficiency
λ_{SOFC}	air-fuel ratio of SOFC

Subscripts

j	subvolume element

The exergy analysis of a combined internal methane reforming-solid oxide fuel cell-gas turbine (IRSOFC-GT) power generation system was performed by Pegah [10]. The in situ partial oxidation of methane and the electrochemical oxidation of hydrogen at the cell anode were taken as main reactions. Fuel cell off gas was used to feed a turbine fulfilling in this way the power requirements for fuel compression. The thermodynamic losses in each unit were calculated and no thermal integration strategy was taken into consideration to exploit the hot sources and minimize the heat use in the system.

In a similar work Calise et al. [4] carried out the simulation and exergy analysis of a hybrid solid oxide fuel cell-gas turbine (SOFC-GT) power system fueled with methane. Energy and exergy balances were performed not only for the whole plant but also for each component in order to evaluate the distribution of irreversibility and thermodynamic inefficiencies. Results showed that, for a non-thermal integrated 1.5 MW system, an electrical efficiency close to 60% can be achieved using appropriate values of the most important design variables. The global efficiency was at about 70% considering the heat recovery.

The use of renewable fuels coupled to SOFCs have been also reported by Panopoulos et al. [11,12] and Fryda et al. [13] which studied the exergy efficiency of a biomass steam gasification reactor integrated with a high temperature SOFC in a combined heat and power scheme. The system operates under optimum conditions for a fuel utilization factor (U_f) of 0.7; above that value considerable exergy losses were reported; at this condition electrical exergetic efficiency was 32%, while the combined electrical and thermal exergetic efficiency was 35% without applying any strategy for the thermal integration and optimal heat use in the system. The CH_4 conversion and CO shift reactions were taken into consideration to take place within cell anode and only electrochemical hydrogen oxidation was assumed.

In the present paper, the first and second laws of thermodynamics are combined to analyze an external catalytic ethanol steam reformer coupled to a solid oxide fuel cell system, starting from the results presented in two papers published previously [7,14]. The system combines the renewable character of ethanol with the technical advantages of fuel cells to design a near zero emission system with a high degree of efficiency. The CO_2 produced in the reforming and in the post-combustion units is absorbed by the biomass in growth (Eqs. (2)–(5)):

$$6CO_2 + 6H_2O \rightarrow C_6H_{12}O_6 + 6O_2\text{: Photosynthesis} \quad (2)$$

$$C_6H_{12}O_6 + ADP \rightarrow 2C_2H_5OH + 2CO_2 + 2ATP\text{ : Fermentation} \quad (3)$$

$$C_2H_5OH + 3O_2 \rightarrow 2CO_2 + 3H_2O\text{ : Ethanol Combustion} \quad (4)$$

$$C_2H_5OH + 3H_2O \rightarrow 2CO_2 + 6H_2O\text{ : Ethanol Steam Reforming} \quad (5)$$

A novel thermodynamic model for the evaluation of the SOFC is provided and a kinetic model is used to asses the conversion of methane within cell anode which is fed with the reformate gas produced in an ethanol steam reforming unit. A detailed model of all components of the plant is introduced, with a special attention to the kinetics of the ethanol steam reforming. Based on this model, the effect of the fuel cell and the reforming operational parameters (reactor temperature, reactants ratio and fuel utilization coeffi-

cient) on the process is presented, in terms of the performance (efficiency and exergy destruction) of the overall system. Also the distribution of irreversibility on each device and the whole process are reported joined to the exergy and energy efficiencies. The study starts with an integrated process flow diagram as base case [14] and all the analysis is developed taken into account the effect of the heat exchanger network (HEN) design throw pinch methodology.

The data and the methodology presented in the present paper can be used to address the analysis of any SOFC-Biomass system based upon thermo-conversion of the primary fuel and the heat integration of the process.

A mathematical model has been developed in order to simulate all processes involved and it is carried out using the Aspen-Hysys® general purpose modeling-environment.

2. Description of the systems

The ethanol steam reformer-solid oxide fuel cell systems is depicted in Fig. 1. The initial fluxes of water and ethanol are pumped into the *mixer* where an isothermal mixing takes place at atmospheric conditions (298 K and 1 atm). After that, the liquid mixture is vaporized and preheated on devices HEX-1 and HEX-2 prior to the *reactor* inlet. The endothermic steam reforming of the ethanol (ΔH = +173.5 kJ/mol) is studied considering a packed bed reactor charged with a Ni/Al hydrotalcite catalyst [15,16] and among the various reaction patterns reported previously [14,16,17] the Langmuir–Hishelwood kinetic model reported in Arteaga et al. [7,14] is used to describe a six step reaction scheme including the coke deposition on catalyst surface (Eqs. (6)–(11)):

$$C_2H_5OH \rightarrow CH_4 + CO + H_2 \quad (6)$$

$$CO + H_2O \rightarrow CO_2 + H_2 \quad (7)$$

$$CH_4 + H_2O \rightarrow CO + 3H_2 \quad (8)$$

$$CH_4 + 2H_2O \rightarrow CO_2 + 4H_2 \quad (9)$$

$$2CO \rightarrow C + CO_2 \quad (10)$$

$$C + H_2O \rightarrow CO + H_2 \quad (11)$$

The mixture leaving the *reactor* is then fed into a solid oxide fuel cell module where an air flux (21% O_2, 79% N_2) which is previously compressed and heated in a *Compressor*, HEX-3 and HEX-4, is used as oxidant. The fuel cell depleted gases react into a *post-combustion* unit to fulfill the energy requirements of the process. The operating conditions of some streams of main process flow diagram (PFD) are shown in Table 1.

It is worth to explain that the base case PFD varies with the change on reactor temperature. The main modification consists in a heat exchanger placed between the cell and the reformer to fulfill the operating condition of the solid oxide fuel cell.

3. Plant analysis: mathematical approach

3.1. Plant capacity

The system is evaluated to produce up to 700 kW of electricity, since SOFC delivered power is ranged between 1 kW to few MW. The initial flows of hydrogen and ethanol are calculated starting from the correlations of continuous current and the Faraday's law, assuming a cell voltage of 0.6 V and an efficiency of 40.5% [1].

For a parallel arrangement:

$$I_{SOFC} = \frac{P_{SOFC}}{V_{SOFC}} \quad (12)$$

Considering the fuel utilization coefficient effect, the necessary theoretical hydrogen is:

$$F_{H_2} = (A)\left(\frac{1\,C\,s^{-1}}{1\,A}\right)\left(\frac{1\,mol\,e^-}{96,487\,C}\right)\left(\frac{1\,mol\,H_2}{2\,mol\,e^-}\right)\left(\frac{3600\ s}{1\,h}\right)\left(\frac{1}{U_f}\right) = mol/h \quad (13)$$

The quantity of ethanol to be feed to the reforming stage and process effectiveness are computed by means of the hydrogen yield and selectivity criterion (Eqs. (14a) and (14b)). The hydrogen yield is defined as the ratio of hydrogen molar flow produced in the reforming reactor and the ethanol molar flow feed to this stage. While selectivity is defined as the quantity of product obtained, times the converted reactants. See Arteaga et al. [24] and

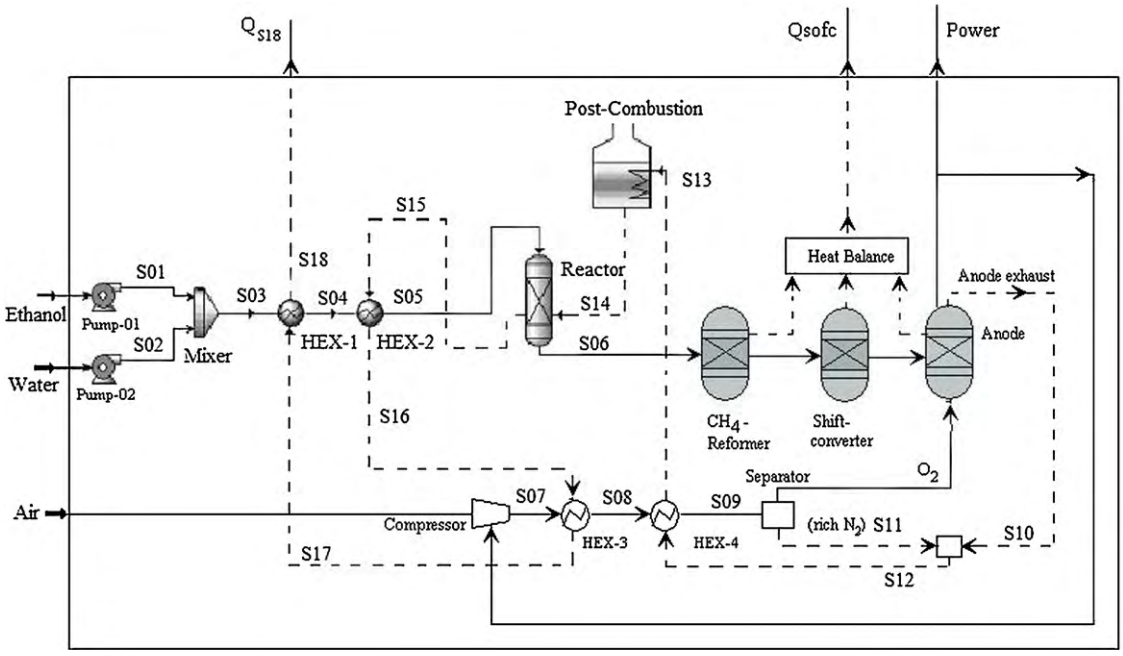

Fig. 1. Process flow diagram and solid oxide fuel cell performance model (PFD).

Table 1
Mass balance summary. Base case: $T_{ESR} = T_{SOFC} = 923$ K, $R_{A/E} = 6.0$.

Name	S03	S05	S06	S09	S10	S11	S12	S13	S14
Temperature (K)	298.15	923.15	923.15	873.14	1023.15	1023.15	1023.15	823.15	1132.27
Pressure (kPa)	101.32	101.32	101.32	121.59	101.32	101.32	101.32	101.32	101.32
Molar flow (kmol/s)	7.6×10^{-3}	7.6×10^{-3}	1.17×10^{-2}	3.2×10^{-2}	1.2×10^{-2}	3.0×10^{-2}	4.2×10^{-2}	4.2×10^{-2}	4.2×10^{-2}
Molar composition (mole fraction)									
C_2H_6O	0.143	0.143	0	0	0	0	0	0	0
H_2O	0.857	0.857	0.338	0	0.7207	0	0.2044	0.2044	0.2385
CO	0	0	0.047	0	0.0465	0	0.0133	0.0133	0.0014
CO_2	0	0	0.129	0	0.1320	0	0.0375	0.0375	0.0512
CH_4	0	0	0.0064	0	0.0030	0	0.0008	0.0008	0
H_2	0	0	0.478	0	0.0976	0	0.0277	0.0277	0
N_2	0	0	0	0.79	0	0.8510	0.6097	0.6097	0.6219
O_2	0	0	0	0.21	0	0.1489	0.1066	0.1066	0.0869
Coke	0	0	0.0016	0	0	0	0	0	0

Fierro et al. [18]:

$$Y_H = \frac{F_{H_2}}{F^{in}_{ethanol}} \tag{14a}$$

$$S_i = \frac{f_i}{f^{in}_{ethanol} - f^{out}_{ethanol}} \tag{14b}$$

The previously mentioned approximations are merely used for the initial guess, because both, the system simulation and integration are trial and error procedures. Also the cell voltage is highly influenced by the irreversibility losses and the operational conditions. If the flows of hydrogen and ethanol are fixed the system indicators could lead to high deviations of the real behavior.

3.2. Ethanol steam reforming

The conversion of water/ethanol mixture is supposed to be carried out in a fixed bed reactor following the reaction scheme presented by Eqs. (6)–(11). Previous thermodynamic studies [19,20] show that ethanol steam reforming (ESR) is feasible to high temperatures ($T > 650$ K) and in a wide range of water/ethanol molar ratios, producing CH_4, H_2O, CO, CO_2 and H_2 as main species. The approach of assuming equilibrium leads to deviations from the real behavior of the reaction and synthesis gas composition [21,22], because the catalyst formulation and the kinetic pattern also play an important role. This problem affects not only the quantification of the reaction parameters but also the accuracy of the process evaluation, due to this, the use of accurate kinetic models is the most feasible route to perform the integration between the ethanol steam reforming and the other sub-systems such as fuel cell and post-combustion.

In the present paper a novel multi-reaction pathway used in conjunction with a Langmuir–Hinshelwood kinetic model based on the mechanistic description of all reaction steps, allows obtaining a detailed concentration profile at the reactor outlet and defining the potential for energy savings, considering the contribution of each component in the reformate gas; see Arteaga et al. [7,14].

The reactor flow field is modeled as plug flow, that is to say, the stream is isotropic in the radial direction (without mass or energy gradients) and axial mixing negligible (Eq. (15)). This implies that the model does not allow studying the radial internal profiles of temperature and concentration:

$$\frac{df(z,i)}{dz} = A_t(1-\varepsilon)\sum_i \alpha(i,j)\cdot r(z,i) \tag{15}$$

where A_t is the flow area (m^2), ε is the porosity, $r_{(z,i)}$ is the reaction rate for component i at the position z (kmol s^{-1} m^{-3}) and $\alpha_{(i,j)}$ is the stoichiometric coefficient for component i, within the reaction j.

The reformer heat duty for each operational condition is rigorously calculated using local film coefficients and the overall heat transfer coefficient definition (Eq. (16)) [14]:

$$Q = U \times \mathrm{Atc} \times (T^{in} - T^{out}) \tag{16}$$

Here: Q is the heat duty (kW), Atc is the heat transfer area (m^2) and U is the overall heat transfer coefficient (kW m^{-2} K^{-1}).

The reactor is supposed to be operated near isothermal conditions, and the energy to drive the endothermic reactions is controlled by external heating through the tube wall. The main geometrical parameters were reported in a previous work [7]. Temperature and water/ethanol molar ratios are considered as the most important operational variables in the analysis based upon previous results reported elsewhere [7,14,18–20].

3.3. Solid oxide fuel cell

A generalized steady-state model is used in order to investigate the performance of a SOFC coupled to an ESR reactor [23,24]. A high operation temperature (923 K) is chosen in order to favor the in situ methane steam reforming, shift reaction and to increase the enthalpy of the exhausted gas.

3.3.1. Performance model

The SOFC model represented in Fig. 1 is used to study the process and to design various scenarios considering variations of the fuel cell and reformer operational parameters. The cell anode is simulated as a series of kinetic, equilibrium and conversion reactors modeled in Aspen Plus.

Since the *S*/*C* ratio of the syngas fed into the anode is higher than two, no carbon deposition problems are supposed to occur on the anode of the SOFC and the in situ methane reforming. Eq. (8) is studied using a kinetic reactor model which considers the power law pattern with a negative reaction order for water [23] (Eq. (17)). Moreover, the shift conversion of the carbon monoxide (Eq. (7)) is simulated using a Gibbs reactor model (*equilibrium*), in this way the offgas composition is calculated rigorously and the energy recuperation in the post-combustor agrees with the real picture of the problem:

$$r_{CH_4 in} = K_{in} \cdot p_{CH_4}^{0.85} \cdot p_{H_2O}^{-0.35} \cdot \exp\left(\frac{-E_{in}}{RT_s}\right) \quad (17)$$

where K_{in} $(8542.0\,\text{mol}\,\text{m}^{-1}\,\text{s}^{-1}\,(\text{bar}_{abs}^2)^{-1}$ is the pre-exponential factor, T_s (K) is the solid surface temperature, E_{in} $(95{,}000\,\text{J}\,\text{mol}^{-1})$ is the activation energy, $p(CH_4)$, $p(H_2O)$ are the partial pressures of methane and water in bar_{abs}, and $r_{CH_4 in}$ $(\text{mol}\,\text{m}^{-1}\,\text{s}^{-1})$ is the reaction rate for the internal methane reforming.

The air and fuel flows are brought to operating pressure and temperature using (*compressor and heatx*) blocks. The oxygen consumed in the electrochemical reaction is separated from the air using a (*separator*) block and the inlet flow of air is calculated for an oxygen stoichiometry of two, representing a utilization of 50% [1]. The fuel utilization factor defined by (Eq. (18)) is varied from 70% to 90%. The heat balance in the cell considers the heat consumed in the methane reforming and the heat produced by the electrochemical reaction and shift conversion:

$$U_f = \frac{f_{H_2}^{in} + 4 \cdot X_{CH_4} \cdot f_{CH_4}^{in} + X_{CO} \cdot f_{CO}^{in} - f_{H_2}^{out}}{f_{H_2}^{in} + 4 \cdot X_{CH_4} \cdot f_{CH_4}^{in} + X_{CO} \cdot f_{CO}^{in}} \quad (18)$$

3.3.2. Electrochemical model

The total cell stack current and the Nernst potential (V_{ideal}) are calculated assuming the principles depicted in Francesconi et al. [21] and Arteaga et al. [14]. All partial pressures involved in the electrochemical model are averaged values between the inlet and outlet of the anode and cathode, respectively. Other important parameter is the current density (J) and it is calculated for an active surface (S_{SOFC}) of 100 m^2 Eq. (19):

$$J = \frac{I_{SOFC}}{S_{SOFC}} = \frac{2F \cdot \left[(f_{H_2}^{in} + 4 \cdot X_{CH_4} \times f_{CH_4}^{in} + X_{CO} \cdot f_{CO}^{in}) - f_{H_2}^{out}\right]}{S_{SOFC}} \quad (19)$$

The actual cell voltage (V_{SOFC}) and power (P_{SOFC}) are estimated using the V_{ideal} and considering the irreversibility losses which mainly occur due to concentration, activation and ohmic overpotentials:

$$V_{SOFC} = V_{ideal} - \eta_{act} - \eta_{conc} - \eta_{ohm} \quad (20)$$

$$P_{SOFC} = I_{SOFC} \cdot V_{SOFC} \quad (21)$$

The activation overpotential is related to the electrode kinetics at the reaction site and the relationship between overpotential and current density can be expressed by the Butler–Volmer equation [24], which for a typical SOFC is expressed as:

$$\eta_{act} = \left(\frac{RT}{F}\right) \sinh^{-1}\left(\frac{J}{2J_{o,i}}\right), \quad i = a, c \quad (22)$$

This expression is valid when two electrons are transferred in the electrochemical reaction and the symmetric factor of the SOFC (alpha) is 0.5 [3,4,24]. The influence of the operational parameters on the exchange current density (J_o) and the activation overpotential at the cathode and anode in the SOFC is studied using the expressions previously reported in Ni et al. [24] and Arteaga et al. [14].

On the other hand, the concentration overpotential is evaluated considering the limit current density, defined by Wang (Eq. (23)) [25]. This parameter is closely related to the transport properties of the fuel and oxidant and the morphological characteristics of the cell electrodes:

$$\eta_{conc} = \frac{RT}{nF} \ln\left(1 - \frac{J}{J_l}\right) \quad (23)$$

The effect of the Ohmic overpotential on the cell voltage is calculated using the equation presented by Ni et al. [24].

3.4. Post-combustion unit

The SOFC exhaust containing H_2, CH_4, O_2, N_2, CO, H_2O, and CO_2 is cooled (to avoid NO_x formation) and burned downstream in the post-combustion system. The post-combustion unit is modeled as an adiabatic conversion reactor (ConvReact) and the depleted heat is used to balance the energy requirements in the process.

The operational conditions (feed temperature, pressure and air excess) of the after burner are taken into account in the system analysis and the model considers three stoichiometric reactions (Eqs. (24)–(26)):

$$H_2 + (1/2)O_2 \rightarrow H_2O : \text{Hydrogen Combustion} \quad (24)$$

$$CO + (1/2)O_2 \rightarrow CO_2 : \text{Carbon Monoxide Combustion} \quad (25)$$

$$CH_4 + 2O_2 \rightarrow CO_2 + 2H_2O : \text{Methane Combustion} \quad (26)$$

4. Second law analysis

Exergy analysis is a thermodynamic method of using the conservation of mass and energy principles together with the second law of thermodynamics for the design and analysis of thermal systems. The purpose of an exergy analysis is generally to identify the location, the source, and magnitude of true thermodynamic inefficiencies in a given process. Exergy is the maximum work that can be produced when a heat or material stream is brought to equilibrium in relation to a reference environment. In this study a temperature of T_o = 298.15 K, pressure P = 1.013 bar and the atmosphere composition of 75.67% N_2, 20.35% O_2, 0.03% CO_2, 3.03% H_2O and 0.92% Ar are assumed as reference state [26].

In the present paper the exergy of the material streams is expressed as the sum of two components, physical and chemical; more precisely, the physical exergy expresses the useful work that a substance can produce when brought reversibly from its state to the "restricted dead state" and it can be written as:

$$e^{ph} = \sum_{i=1}^{n} (H - H_o)_i - T_o(S - S_o)_i \quad n = S01, S02, S03, \ldots, S0n \quad (27)$$

Chemical exergy is obtained when the components of the energy carrier are first converted to reference compounds and then diffuse into the environment, which is in the reference (dead) state. For a gaseous stream flow, the molar chemical exergy (e_i^{ch}) of all species is given by the Eq. (28) [13]:

$$e^{ch} = \sum x_i \cdot e_i^o + RT_o \sum x_i \cdot \ln(x_i) \quad (28)$$

No deviations between real environmental and reference conditions are considered. The standard chemical exergies of all components of each stream represented in the PFD are showed in Table 2.

An exergy balance for a control volume at steady state is formulated to calculate the exergy destruction (E_{irrev}) of the system at different operational conditions. In the present work all the inlet and outlet streams are considered to determine the irreversibility distribution, which includes the sum of matter, energy and power. The *mixer*, *heat exchangers* (HEX-1–HEX-6), ethanol steam reforming *reactor*, the *SOFC* module, the *post-combustion* unit and the auxiliary equipments (pumps and compressor) are included into the limits of the system (external square area in Fig. 1). The process global exergy balance, by ignoring the changes in kinetic and potential exergies, is expressed as:

$$E_{irrev} = \left(\sum f_i \cdot e_i\right)_{inlet} - \left(\sum f_i \cdot e_i\right)_{outlet} + \sum_j \left(1 - \frac{T_o}{T_j}\right) Q_j - W \quad (29)$$

where $E_{irrev} = T_o{}^* S_{gen}$ (the Gouy–Stodola theorem) represents the rate of exergy destruction into the device due to irreversibilities, e_i is the total exergy of each chemical species i, which is the sum of the physical and chemical exergies.

4.1. Definition of the irreversibilities

Irreversibility at each stage of the process is calculated based on the approaches described previously. The equations for the evaluation of this parameter are presented below.

4.1.1. Steam reforming reactor

Exergy destruction of the ESR can be expressed by the following equation:

$$E_{ESR} = (f_{S05} \cdot e_{S05} + f_{S14} \cdot e_{S14} - f_{S06} \cdot e_{S06} - f_{S15} \cdot e_{S15}) \quad (30)$$

Table 2
Standards chemical exergy (Stds. Chem. Exergy) of species (i) [26].

Species	Formula	Stds. Chem. Exergy
Nitrogen	N_2	720
Oxygen	O_2	3970
Water	H_2O_g	1.171×10^4
Water	H_2O_l	3120
Carbon dioxide	CO_2	2.014×10^4
Carbon monoxide	CO	2.754×10^5
Argon	Ar	1.169×10^4
Ethanol	$C_2H_5OH_g$	1.371×10^6
Ethanol	$C_2H_5OH_l$	1.365×10^6
Methane	CH_4	8.365×10^5
Hydrogen	H_2	2.385×10^5
Carbon	C	4.108×10^5

Note: All the exergy values are presented in kJ kmol^{-1}.

4.1.2. Heat exchanger equipment

The exergy balances in all heat exchanger devices can be expressed as follows:

$$E_{HEX_j} = \left(1 - \frac{T_o}{T_j}\right) Q_j + f_{hot}\left[(e_i^{ph})_{inlet} - (e_i^{ph})_{outlet}\right]_{hot} + f_{cold}\left[(e_k^{ph})_{inlet} - (e_k^{ph})_{outlet}\right]_{cold} \quad (31)$$

where j, i, k are 1, 2, 3, 4, . . ., n for heat exchangers HEX-1 to HEX-n.

The previous equation is not affected by chemical exergy due to the chemical compositions of the hot and cold inlet streams are constants in the heat exchange equipment.

4.1.3. Solid oxide fuel cell

The chemical transformations into the fuel cell cathode and anode, the dissipated heat to the environment and the power delivered by the electrochemical reaction are considered into the irreversibilities. Then the exergy destruction in the SOFC is calculated as below:

$$E_{SOFC} = -\left(1 - \frac{T_o}{T_{SOFC}}\right) Q_{SOFC} - P_{SOFC} + \sum [(f_{S09} \cdot e_{S09} - f_{S11} \cdot e_{S11})]_{cathode} + \sum [(f_{S06} \cdot e_{S06} - f_{S10} \cdot e_{S10})]_{anode} \quad (32)$$

4.1.4. Compressor

The expressions to determine the compressor and turbine irreversibilities are reported by Pegah [10]. It takes into account the compression or expansion ratios, polytropic efficiencies and fluid conditions:

$$E_C = f_{air} \cdot R \cdot T_o \left(\frac{1 - \eta_{p,c}}{\eta_{p,c}}\right) \cdot \ln(CPR) \quad (33)$$

4.1.5. Post-combustion unit

In the after burner the irreversibility is defined considering the chemical and physical components, the losses by heat transfer are zero because the combustor operates adiabatically:

$$E_{PC} = (f_{S13} \cdot e_{S13}^{ch} - f_{S14} \cdot e_{S14}^{ch}) + [(f_{S13} \cdot H_{S13} - f_{S14} \cdot H_{S14})T_o(f_{S13} \cdot S_{S13} - f_{S14} \cdot S_{S14})] \quad (34)$$

5. System energy and exergy efficiencies

Energy efficiency of the whole system (Eq. (35)) is defined by the ratio between the delivered power and the amount of energy contained in the ethanol molecular structure it is referred to the LHV. A more detailed description can be consulted in Hernandez et al. [27]:

$$\eta_{energy} = \frac{\sum_j W_j}{(f^{in} \cdot LHV)_{ethanol}} \quad (35)$$

where $\sum_j W_j$ is the global power generated by the system (work produced – work consumption).

On the other hand, exergy efficiency (Eq. (36)) is referred to the exergetic potential of the primary fuel (*standard exergy of ethanol*):

$$\eta_{exergy} = \frac{\sum_j W_j}{(f^{in} \cdot e^o)_{ethanol}} \quad (36)$$

6. Results and discussion

6.1. Effect of the operation parameters on ethanol steam reforming unit

The effect of temperature and water to ethanol molar ratio on hydrogen yield is presented in Fig. 2.

Previous thermodynamics studies have stated that the most feasible molar ratios (R_{AE}) for the hydrogen production using ethanol steam reforming are near to 10:1 at atmospheric pressure and high temperatures ($T > 823$ K) [19,20]. But those works do not take into account the effect of this variable on the whole system performance. In the present work molar ratios ranging between 5:1 and 6.5:1 were explored considering the results obtained in previous papers [7,14].

Even when high reagent ratios favor the hydrogen production (yield = 5.43 at $R_{AE} = 6.5$ and $T = 973$ K), the excess in the water flows includes an extra energy demand which is mainly located at the vaporization and heating stages ($Q \sim 612.64$ kW at 923 K and $R_{AE} = 6.5$). This demand is partially fulfilled by the hot and cold streams in the process but includes an efficiency penalty [21].

On the other hand, smaller amounts of water ($R_{AE} < 3.0$) produce a fall of the hydrogen concentration in the synthesis gas stream and an increase in the coke deposition on the catalyst surface. Those phenomena do not only affect the catalyst performance but also the efficiency on the fuel cell and heat transfer recovery, since the lower content of hydrogen in the cell inlet produces a proportional decrease in the delivered power and the LHV of the anode exhaust gases [14,21,22].

As can be corroborated in Fig. 2, the hydrogen yield is strongly improved when the reactor temperature is increased from 823 K to 973 K. As was discussed in two previous papers [7,14] the ethanol decomposition and the methane steam reforming are promoted, mainly due to the effect of temperature on kinetics and equilibrium respectively. More specific, the methane reforming (Eqs. (8) and (9)), is an endothermic equilibrium process which is highly favored by the increment of temperature [1,28] and also by water to ethanol molar ratios (Le Châtelier–Braun principle). An increment of temperature makes the equilibrium to be established at such a condition where hydrogen production increases as it is show bellow.

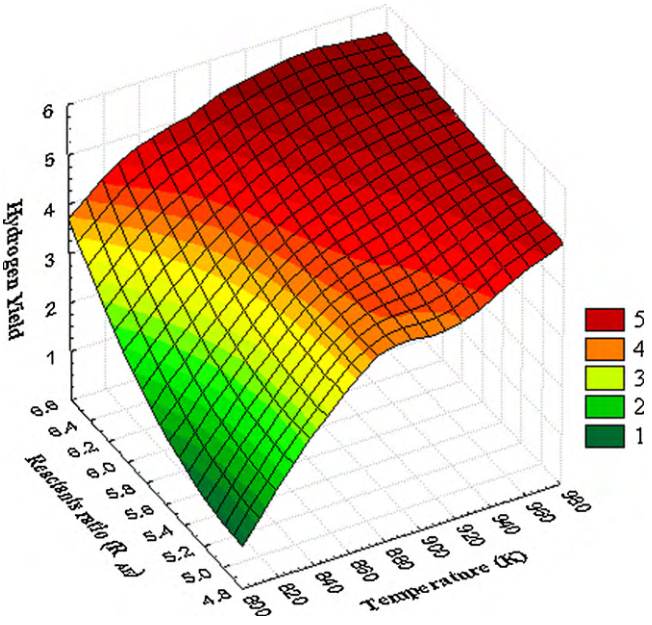

Fig. 2. Effect of temperature and water/ethanol molar ratio on hydrogen yield ($mol_{H_2}/mol_{Ethanol}$).

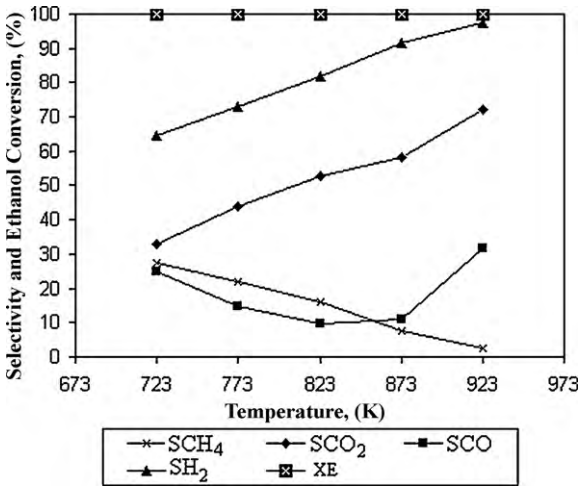

Fig. 3. Effect of the temperature on ethanol conversion and selectivity of each component.

Moreover the carbon monoxide production rises slightly when the temperature overcomes the 823 K because of the reverse water gas reaction (RWGSR), which can be corroborated in Fig. 3; but the SOFC fuel cell runs properly at those concentration levels (CO ~ 5%). Besides the remaining CO (LHV = 50.9 MJ/kg) can be burned in the post-combustion unit to fulfill the energy requirements in the process. If the SOFC is replaced by a low temperature device such as polymeric fuel cells (PEMFC) the concentration of CO must be reduced using additional purification stages such as WGSR and preferential CO oxidation.

Summarizing the discussed above, it can be stated that the increase in the water content:

- Increases the reaction yield.
- Increases the heat consumption at the conditioning stages.
- Superimposes a higher exhaust reuse.
- Favors the equilibrium of methane reaction at the reformer.

It is worth to say that the subsequent study of energy and exergy behavior of the system, will consider the effect of water to ethanol molar ratios as in the reforming stage as for the whole process performance.

6.2. Analysis of the SOFC running on synthesis gas

The polarization curve of a solid oxide fuel cell working on synthesis gas is shown in Fig. 4. The operating conditions of the fuel cell entering gas are deduced from stream S09 and reported in Table 1 (a typical reformate gas composition: 47% H_2, 34% H_2O, 4.7% CO, 12.9% CO_2 and 0.67% CH_4), but without considering coke presence because it is assumed that the generated coke at the reforming reaction is deposited in the catalytic surface.

The activation overpotential for the cathode is higher than for the anode due to its lower exchange current density. The gradual increase in the activation overpotential is less drastic at higher current densities (>10,000A m^{-2}) while the ohmic overpotential increases steeply for the whole range. It is important to point out that the structure and design of the fuel cell could lead to different polarization curves as the operational parameters of cell and reforming gas composition can affect the system performance.

Fig. 5 reports the cell voltage and the total delivered power of the stack for different current densities and fuel utilization factors. The analyzed fuel utilization factor ranges from 70% to 90% since

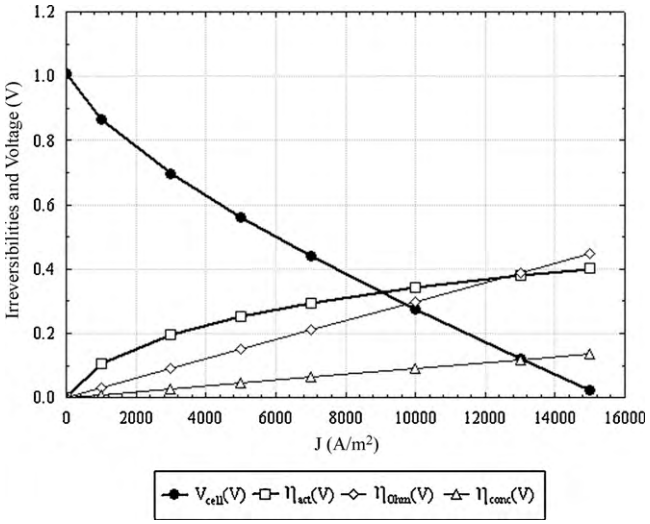

Fig. 4. Solid oxide fuel cell polarization curve. $T = 923$ K and $R_{AE} = 6$.

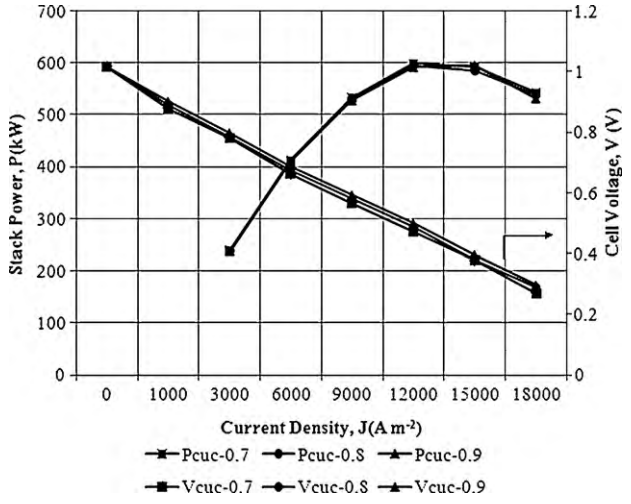

Fig. 5. Cell voltage and the total delivered power of the stack at different current densities and fuel utilization factors (U_f).

to excessive low values of this parameter lead to lower efficiencies on the cell and very higher values also result into efficiency losses and very low energy content in the fuel cell exhaust gas, affecting in this way the recovery of energy at the post-combustion unit and an unbalance for the system utilities.

If Fig. 5 is carefully analyzed a lower voltage for fuel utilization coefficient of 90% is found at all the explored current densities. This behavior was previously reported by Panopoulos et al. [11,12] and Ni et al. [21] and is closely related with the Nernst potential and overpotential definitions. In the present paper the analysis leads with hydrogen electrochemical conversion, water gas shift and in situ methane reforming on fuel cell electrodes. Increasing U_f results in high activation and ohmic overpotentials due to hydrogen and oxygen partial pressure decrease at the cell outlet.

The behavior of the power delivered can be explained considering the previous mentioned and analyzing the proposed model for the SOFC. The maximum electric power output (near to 600 kW)

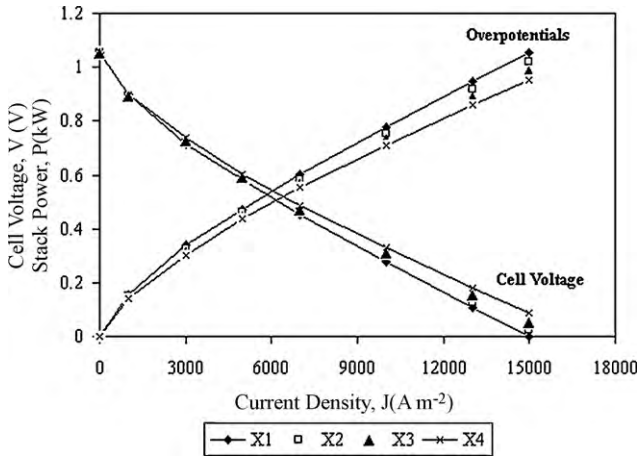

Fig. 6. Effect of reforming gas composition on cell voltage. *X*1, *X*2, *X*3 and *X*4 correspond to reactants molar ratios of 5, 5.5, 6 and 6.5 respectively.

occurs at higher current densities because of the lower activation overpotentials. Nevertheless working at very low values of U_f will include an efficiency penalty.

The effect of reforming gas composition on cell voltage and stack power is reported in Fig. 6. The use of a three reaction model to describe the fuel cell and an excess of water in the reforming stage, makes feasible the conversion of remaining CH_4 and CO at the cell electrodes; due to this, the effect of variations of reforming gas composition have a negligible influence on cell voltage and overpotential.

Singhal and Kendall [29] have reported that the in situ reforming and shift reaction makes the fuel composition variation less important to the cell performance and only considerable deviations are reported for different fuel sources (alcohols, biogas, ethanol, methane).

7. Exergy analysis considering operation parameters

An exergy study has been developed in order to simulate the power plant using the solid oxide fuel cell technology represented in Fig. 1. This simulation program is able to calculate the flow rate, temperature, pressure, energy and the exergy content in every stream of inlet and outlet as well as the exergy destruction by irreversibilities of each stage involved in the plant.

The results of the exergy analysis applied to the base case are shown in Table 3. The conditions selected were $T_{ESR} = T_{SOFC} = 923$ K, $R_{AE} = 6.0$, $U_f = 80\%$, $V_{cell} = 0.64$ V, compressor polytrophic efficiency $\eta_{p,c} = 90\%$ and $\lambda_{SOFC} > 2$. Considering the standard chemical potential of ethanol as the inlet flow availability, the irreversibilities represent approximately 66% of the flow availability, so the exergy efficiency takes a value of 34%.

The increment of the fuel utilization coefficient has a direct effect on system exergy efficiency and irreversibilities. As it is presented in Fig. 7, the increment of fuel utilization allows the fuel cell to produce a higher quantity of delivered power, due to the anode reactions are verified in a higher extension. However, there is no reason to work at U_f of 90%, because the improvement of the efficiency with respect to $U_f = 80\%$ is merely at about 2% while the irreversibilities are ~660 kW higher than those obtained at $U_f = 80\%$ at a constant reforming temperature. The negative effect on irre-

Table 3
Base case simulation results.

Cell voltage	Inlet flow availability	Stack power	Net power	Energy efficiency	Exergy efficiency
0.64 V	1480.79 kW	569.92 kW	502.24 kW	37.64%	33.92%

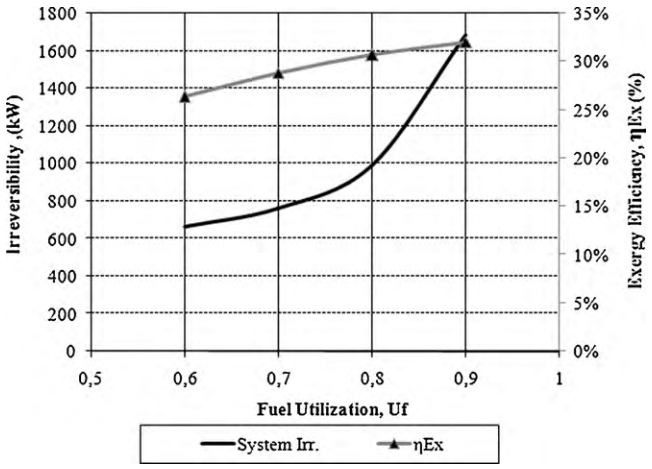

Fig. 7. Effect of fuel utilization coefficient on system irreversibilities and exergy efficiency. $T = 923$ K and $R_{AE} = 6.0$.

versibilities is caused by:

(a) At $U_f > 80\%$, the flow of oxidant entering the SOFC is increased and because of this, the work consumed by the compressor is also incremented.
(b) While U_f is increased the energy content of the exhaust gas is reduced and the system heat balance is affected, being necessary to add an extra ethanol quantity (612 mol/h) to fulfill the leak of auto-sustainability Akkaya et al. [30].
(c) The released heat by the fuel cell was considered as a waste; this heat is also incremented with the reaction extent as well as U_f, similar results are reported by Douvartzides et al. [9].
(d) Increasing fuel utilization factor results in a reduction of fuel flow rate entering module and an increase of voltage losses due to polarizations.

It is important to say that the definition given in this paper for the fuel utilization factor (Eq. (17)) is also affected by the reforming operation parameters such as reaction temperature and water to ethanol ratio which define the *S*/*C* ratio at the cell anode. Because of this, the subsequent sections are devoted to explain the relationship between the fuel cell operation and the R_{AE} and reforming temperature by means of a coupling between an energy and exergy tools.

The effect of the reforming temperature and reactants molar ratio on exergetics efficiency and losses are presented in Figs. 8 and 9 respectively.

The fuel cell power and the ethanol flow have a notable influence on the exergy efficiency according to the definition written previously (Eq. (36)). On the other hand, the cell power is directly proportional to the hydrogen obtained in the reformer. Because of this; the higher hydrogen yield allows the increase of the SOFC power as well as the exergy efficiency. According to the explanation above; the exergy efficiencies are favored by higher reformer temperatures and water to ethanol feed ratios. Exergetic efficiencies reach values ranging from 32% to 35% approximately in all analyses; the higher efficiencies are obtained at 973 K and R_{AE} of 6.5.

From an irreversibility point of view, the system studied is not favored by the increase of the reformer operation variables. The lower irreversibility values are obtained at lower temperature and R_{AE}, nevertheless it corresponds to lower exergy efficiency of the process (less than 30%), and so there should always be a balance between system efficiency and system irreversibility.

Nevertheless the process designer must decide if working at temperatures lower than 973 K allows obtaining a good efficiency

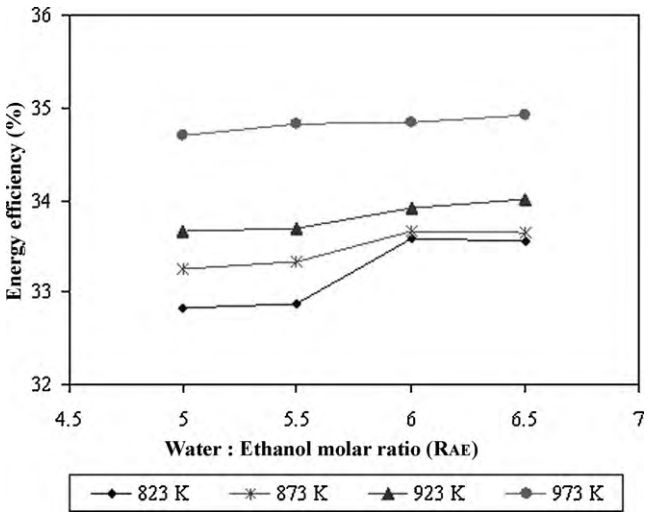

Fig. 8. Effect of the reforming temperature and R_{AE} on exergetic efficiency.

and also improve the security and catalyst durability, due to the higher temperatures favors the catalytic sintering and the use of expensive materials for the reforming tubes. The difference between 973 K and 923 K in efficiency is very low (at about 2%) while the irreversibilities are 60 kW, considering this fact it can be establish the work at 923 K and water to ethanol ratio of 6.5, to achieve a good exergy efficiency (~34%), to fulfill the system requirements and to reduce the coke deposition on catalyst surface [22].

Further on, it is important to express that the flow diagram is designed on integration principles allowing an optimal use of the hot streams and keeping the design of the plant to operate autonomously, without any interaction between external sources of heat and power (auto-sustainability).

The irreversibility of the stages involved in the plant at reforming temperature of 923 K is illustrated in Fig. 10. The total exergy destruction in the system is caused mainly by the SOFC, reformer and post-combustor, which represents more than the 50% of the inlet flow availability, similar results are reported by Pegah [10]. Changes in the chemical exergies are more relevant than the changes of the physical contributions; this phenomenon is related fundamentally with the chemical reactions extents.

The exergy destruction of the reformer is increased from 276.13 kW to 336.53 kW for feed molar ratios of 5 and 6.5 respec-

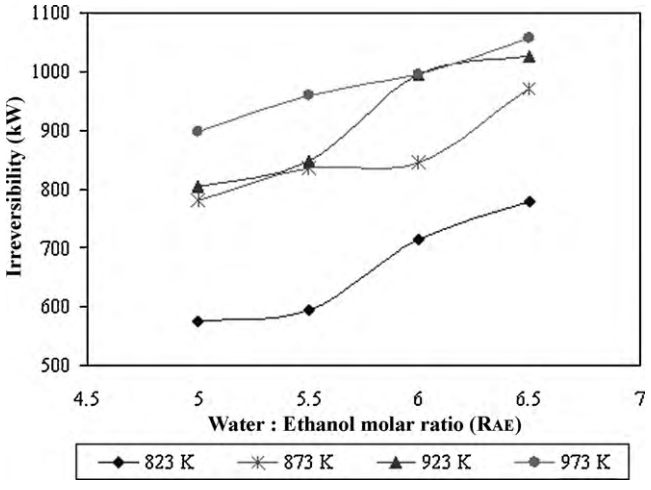

Fig. 9. Irreversibilities, varying the reforming temperature and R_{AE}.

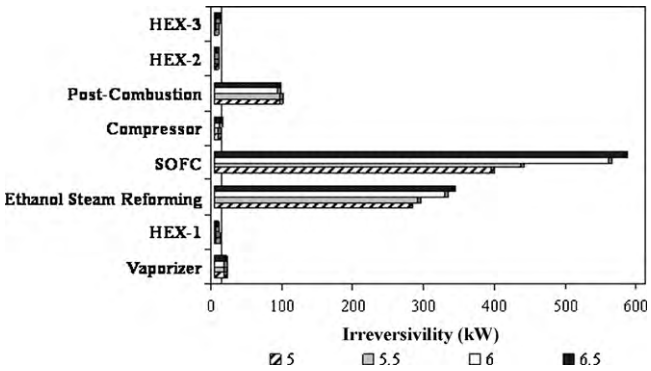

Fig. 10. Exergy destruction by irreversibility in all process stages varying R_{AE}.

tively. That change in performance is due to the increase on the demands of heat in the reformer with R_{AE}, which is caused by the increase of reactions conversion taking place in this stage and the total flow (Eqs. (5)–(10)).

In order to investigate the performance of the exergetic losses in the fuel cell, it is assumed that the heat rejected by the electrochemical reaction is a waste, because of this; the exergy destructions by heat losses are significant, reaching values of 70% of the exergy destruction of the SOFC for water to ethanol molar ratio of 6.5. The efficient use of wasted heat by the cell in a turbine, heat engines or in a combined cycle can reduce the irreversibilities in this stage and the global system, as well as to improve the exergy and energy efficiencies [27].

The increase of R_{AE} produce a higher hydrogen flow to the fuel cell, converting more chemical energy into electricity, which means more current and power produced. Nevertheless at the same condition, the irreversibility is increased in the fuel cell stack due to the increase of the waste heat and dissipative phenomena (overpotential losses).

The exergy destruction in the post-combustor presents a little decrease for different R_{AE}. Those losses are associated to the irreversibility of the combustion process of H_2, CO and CH_4, the amounts of reactants, the temperature of the combustor and the stoichiometric ratio of the combustion. In this case the amounts of fuels take an important role; especially the energetic content of the inlet stream is reduced with the increase of the water to ethanol molar ratio, allowing lower losses by the heat transfer.

8. Conclusions

The evaluation presented in this paper allows obtaining a complete idea of the real work delivered by an integrated solid oxide fuel cell and an ethanol steam reforming unit and it relationship with the most relevant operation variables. The system performance was studied considering a detailed kinetic model for the ethanol steam reforming reported in a previous paper [14] and a complete stationary fuel cell description. The effect of water to ethanol ratio, fuel utilization coefficient and the reforming temperature on the energy and exergy efficiency of the system was also discussed.

The power delivered by the cell exhibits a maximum at some current density (12,000 A m^{-2}) for all the utilization factors explored. The higher exergy efficiencies (35% at 973 K and R_{AE} = 6.5) also coincide with higher total irreversibility losses (1050 kW) due to the effect of the change in both the chemical and physical components. It was also demonstrated that a balance should be established by the process engineer considering equilibrium between power production and process efficiencies.

Acknowledgments

The authors' whish to acknowledge to editor and unknown referees. This work has been financially supported by VLIR Program, Project 7. Environmental Education and Development of Clean Technologies. Ghent University, Faculty of Bioscience Engineering. Arteaga acknowledges the professor Miguel Laborde, the researchers of the Catalytic Productions Laboratory of Universidad de Buenos Aires and the CYTED (Projects 3303 and 332205).

References

[1] J.H. Hirschenhofer, D.B. Stauffer, R.R. Engleman, M.G. Klett, Fuel Cells Handbook, 6th ed., EG & G Technical Services, National Energy Technology Laboratory, Morgantown, WV, 2006.
[2] B. Thorud, Dynamic Modeling and Characterization of a Solid Oxide Fuel Cell Integrated in a Gas Turbine Cycle, Doctoral Thesis, Department of Energy and Process Engineering, Norwegian University of Science and Technology, 2005.
[3] F. Calise, A. Palomb, L. Vanoli, J. Power Sources 158 (2006) 225–244.
[4] F. Calise, A. Palomb, L. Vanoli, Energy 31 (2006) 3278–3299.
[5] Ballard, Case Study—Residential Cogeneration, Groundbreaking Fuel Cell Solution, Ballard Power Systems Inc., British Columbia, 2007.
[6] N. Hotz, S.M. Sen, D. Poulikakos, J. Power Sources 158 (2006) 333–347.
[7] L.E. Arteaga, Y. Casas, L.M. Peralta, V. Kafarov, J. Dewulf, P. Giunta, Chem. Eng. J. 150 (2009) 242–251.
[8] S. Douvartzides, F. Coutelieris, P. Tsiakaras, J. Power Sources 131 (2004) 224–230.
[9] S. Douvartzides, F. Coutelieris, P. Tsiakaras, J. Power Sources 114 (2003) 203–212.
[10] G.B. Pegah, Int. J. Hydrogen Energy 32 (2007) 4591–4599.
[11] K.D. Panopoulos, L. Fryda, J. Karl, S. Poulou, E. Kakaras, J. Power Sources 159 (2006) 586–594.
[12] K.D. Panopoulos, L. Fryda, J. Karl, S. Poulou, E. Kakaras, J. Power Sources 159 (2006) 570–585.
[13] L. Fryda, K.D. Panopoulos, J. Karl, E. Kakaras, Energy 33 (2008) 292–299.
[14] L.E. Arteaga, L.M. Peralta, V. Kafarov, Y. Casas, E. Gonzalez, Chem. Eng. J. 136 (2008) 256–266.
[15] V. Mas, G. Baroneti, N. Amadeo, M. Laborde, Chem. Eng. J. 138 (2008) 602–607.
[16] V. Mas, M.L. Dieuzeide, M. Jobbagy, G. Baroneti, N. Amadeo, M. Laborde, Catal. Today 133–135 (2008) 319–323.
[17] A. Akande, A. Aboudheir, R. Idem, A. Dalai, Int. J. Hydrogen Energy 31 (2006) 1707–1715.
[18] V. Fierro, V. Klouz, O. Akdim, C. Mirodatos, Catal. Today 75 (2005) 141–144.
[19] M.A. Laborde, E.Y. Garcia, Int. J. Hydrogen Energy 16 (1991) 307.
[20] K. VAsudeva, N. Mitra, P. Umasankar, S.C. Dhingra, Int. J. Hydrogen Energy 21 (1996) 13–18.
[21] J.A. Francesconi, M.C. Mussati, R.O. Mato, P. Aguirre, J. Power Sources 167 (2007) 151–161.
[22] P. Giunta, C. Mosquera, N. Amadeo, M. Laborde, J. Power Sources 164 (2007) 336–343.
[23] F.P. Nagel, T.J. Schildhauer, M.A. Biollaz, S. Stucki, J. Power Sources 184 (2008) 129–142.
[24] M. Ni, D.Y.C. Leung, M.K.H. Leung, Int. J. Hydrogen Energy 32 (2007) 3238–3247.
[25] J. Wang, Analytical Electrochemistry, 2nd ed., John Wiley & Sons, 2000.
[26] T.J. Kotas, The Exergy Method of Thermal Plant Analysis, Krieger Publishing Company, Florida, 1995.
[27] L. Hernandez, V. Kafarov, Int. J. Hydrogen Energy, 2008, doi:10.1016/j.ijhydene.2008.07.089.
[28] M.S. Smith, H.C.V. Ness, M.M. Abbot, Introduction to Chemical Engineers Thermodynamics, Chemical Engineers Series, 7th ed., McGraw-Hill, 2005.
[29] A.C. Singhal, K. Kendall, High Temperature Solid Oxide Fuel Cells: Fundamentals, Design and Applications, Elsevier Inc., New York, 2003, ISBN 1856173879.
[30] A.V. Akkaya, B. Sahin, H.H. Erdem, Thermodynamic model for exergetic performance of a tubular SOFC module, Renew. Energy 34 (2009) 1863–1870.